

GaAs nanowire Schottky barrier photovoltaics utilizing Au–Ga alloy catalytic tips

Ning Han, Fengyun Wang, SenPo Yip, Jared J. Hou, Fei Xiu et al.

Citation: *Appl. Phys. Lett.* **101**, 013105 (2012); doi: 10.1063/1.4727907

View online: <http://dx.doi.org/10.1063/1.4727907>

View Table of Contents: <http://apl.aip.org/resource/1/APPLAB/v101/i1>

Published by the [American Institute of Physics](#).

Related Articles

A new architecture for solar cells involving a metal bridge deposited between active TiO₂ particles
J. Appl. Phys. **111**, 123109 (2012)

Bandgap engineering of ZnSnP₂ for high-efficiency solar cells
Appl. Phys. Lett. **100**, 251911 (2012)

High performance dye-sensitized solar cell based on hydrothermally deposited multiwall carbon nanotube counter electrode
Appl. Phys. Lett. **100**, 243303 (2012)

High performance dye-sensitized solar cell based on hydrothermally deposited multiwall carbon nanotube counter electrode
APL: Org. Electron. Photonics **5**, 127 (2012)

Effect of textured electrodes with light-trapping on performance of polymer solar cells
J. Appl. Phys. **111**, 104516 (2012)

Additional information on *Appl. Phys. Lett.*

Journal Homepage: <http://apl.aip.org/>

Journal Information: http://apl.aip.org/about/about_the_journal

Top downloads: http://apl.aip.org/features/most_downloaded

Information for Authors: <http://apl.aip.org/authors>

ADVERTISEMENT

AIP Advances

Special Topic Section:
PHYSICS OF CANCER

Why cancer? Why physics? [View Articles Now](#)

GaAs nanowire Schottky barrier photovoltaics utilizing Au–Ga alloy catalytic tips

Ning Han,¹ Fengyun Wang,² SenPo Yip,¹ Jared J. Hou,¹ Fei Xiu,¹ Xiaoling Shi,¹ Alvin T. Hui,¹ TakFu Hung,¹ and Johnny C. Ho^{1,3,a)}

¹Department of Physics and Materials Science, City University of Hong Kong, Tat Chee Avenue, Kowloon, Hong Kong

²Department of Biology and Chemistry, City University of Hong Kong, Tat Chee Avenue, Kowloon, Hong Kong

³Centre for Functional Photonics (CFP), City University of Hong Kong, Tat Chee Avenue, Kowloon, Hong Kong

(Received 1 May 2012; accepted 22 May 2012; published online 2 July 2012)

Single GaAs nanowire photovoltaic devices were fabricated utilizing rectifying junctions in the Au–Ga catalytic tip/nanowire contact interface. Current-voltage measurements were performed under simulated Air Mass 1.5 global illumination with the best performance delivering an overall energy conversion efficiency of $\sim 2.8\%$ for a nanowire of 70 nm in diameter. As compared with metal contacts directly deposited on top of the nanowire, this nanoscale contact is found to alleviate the well-known Fermi-level pinning to achieve effective formation of Schottky barrier responsible for the superior photovoltaic response. All these illustrate the potency of these versatile nanoscale contact configurations for future technological device applications. © 2012 American Institute of Physics. [<http://dx.doi.org/10.1063/1.4727907>]

Due to the superior electronic transport properties and light-coupling effects, semiconductor nanowires (NWs) such as Si, Ge, and GaAs are widely used as fundamental building blocks for the next generation electronics, optoelectronics, and photovoltaics.^{1–5} The synthesis of those NWs usually adopts a well-established vapor-liquid-solid (VLS) and/or vapor-solid-solid (VSS) mechanism, where metal particles, like the most commonly explored gold (Au) nanoclusters, are utilized for the catalytic growth.^{1,4,6–8} During the NW nucleation and growth, precursor atoms are diffused through these Au catalysts inducing NW formation at the Au/NW interface; therefore, chemical bonds are formed in this abrupt junction yielding nanoscale metal/NW contacts, which are in distinct contrast to “bulk-contacts” with the weak physical interaction between post-growth deposited metal electrodes and NWs.⁹ In bulk contacts, metal-induced gap states often determine the Schottky barrier height in which the interface Fermi level is pinned and no longer moves when metals with different work functions are deposited; in nanoscale contacts, metal-induced gap states are believed to have weaker impact on this pinning due to the electrostatics at reduced dimensions.⁹ In this regard, here, we utilize this nanoscale contact scheme on GaAs NWs with Au–Ga alloy catalytic tips to fabricate Schottky barrier photovoltaic devices. As compared with conventional Schottky device structures with Au contacts directly deposited on top of the NW, the tip-contacted devices result in the much higher solar energy conversion efficiency ($\sim 2.8\%$ under AM1.5G illumination), suggesting the effective formation of rectifying junctions in these nanoscale contact interfaces. Interestingly, when normalized to the light absorption cross-sectional area, the short-circuit current density (J_{sc}) and efficiency (η) are found to scale quasi-linearly with the NW diameters whereas the open-

circuit voltage (V_{oc}) remains relatively constant. All of these further demonstrate the uniform charge transfer or injection across the tip/NW interface and illustrate the technological potency of these nanocontacts for future device applications.

GaAs NWs were prepared by a solid-source chemical vapor deposition (CVD) method as reported previously.¹⁰ Briefly, GaAs powders (~ 2 g) were heated in the upstream zone (900°C) of a two-zone tube furnace and the Ga and As₂ vapors were carried by H₂ (100 sccm) to the downstream zone of the furnace (600°C), where GaAs NWs are grown *via* the VLS/VSS mechanism by using the thermally deposited 20 nm Au thin film on Si/SiO₂ substrate (pre-annealed at 800°C for 10 min) as the catalyst for a growth duration of 60 min. The GaAs NWs were cooled down in H₂ atmosphere and were dispersed in ethanol by sonication. Then the GaAs NWs suspension was dropped onto a copper grid for transmission electron microscopy (TEM) and energy-dispersive x-ray spectroscopy (EDS) analysis. In this work, GaAs NWs were first drop-casted onto Si/SiO₂ (50 nm thermally grown) substrates, followed by the definition of electrodes by photolithography, Ni deposition, and lift-off processes. This way, NWs with catalytic tips (“tipped NWs”) and without tips (cut down by sonication to become “bare NWs”) were randomly distributed into 2 and 5 μm device channels. Importantly, as a comparison, Au electrode was defined by repeating the fabrication processes for the “bare NW” devices to form Ni/NW/Au asymmetric contacts. The fabricated photovoltaic (PV) devices were observed by a scanning electron microscope (SEM) and the corresponding PV performance was measured with an Agilent 4155 C semiconductor analyzer under dark and AM 1.5G illumination (100 mW/cm², Newport 96000 solar simulator).

In the NW synthesis, a spherical catalytic tip is typically observed among the prepared GaAs NWs, growing dominantly in $\langle 111 \rangle$ direction, as shown in Fig. 1(a). From the EDS spectrum taken in the tip region (Fig. 1(b)), the

^{a)} Author to whom correspondence should be addressed. Electronic mail: johnnyho@cityu.edu.hk.

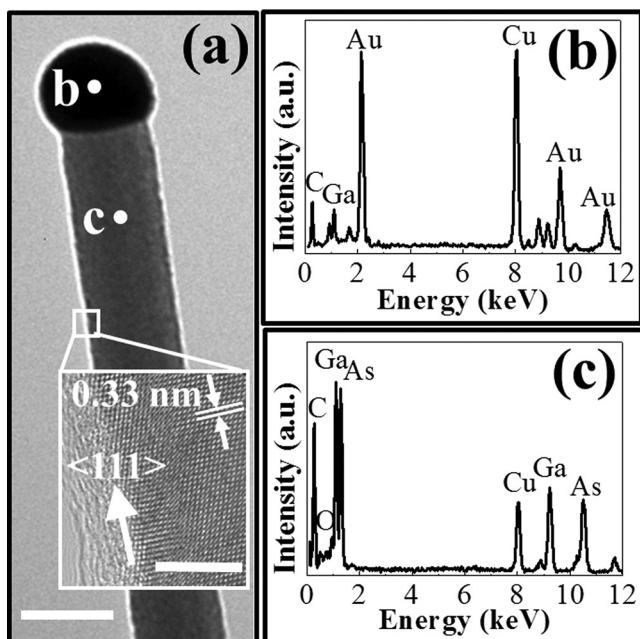


FIG. 1. TEM and EDS results of a typical GaAs NW. (a) TEM image (scale bar = 50 nm) and inset is an HRTEM image (scale bar = 5 nm), showing a typical NW growing in $\langle 111 \rangle$ direction, (b) EDS spectrum of spot b (catalytic tip), and (c) EDS spectrum of spot c (NW body).

catalytic tip is composed mainly of Au and Ga substituents, which agrees well with the reported VLS/VSS growth mechanism that Ga is precipitated from the Au catalyst, while As is diffused through the tip/NW interface and NW sidewall, due to the low solid solubility of As in Au, to yield the NW formation.^{6,7} As depicted in Fig. 1(c), the GaAs NW body is found highly stoichiometric with the Ga/As ratio approximating 1:1, without any detectable Au content within the resolution limit of EDS. Notably, oxygen is also identified in the NW body (~ 10 at. %) which is well-recognized in the VLS/VSS grown GaAs NWs as a result of an amorphous oxide surface layer,^{11,12} in which the oxide layer is further confirmed in the high-resolution TEM image in Fig. 1(a) inset. Since there are abundant interface trapping states between the NW core and the oxide layer,^{13–15} they would also play a key role in the Fermi level pinning of GaAs NWs, in addition to the metal-induced gap states, when contacted with metal electrodes regardless of their difference in the work function.^{16,17} All these mid-gap states would impose substantial

challenges to obtain effective electrical contact with NWs for practical applications.

In order to investigate the above-mentioned nanoscale contact to GaAs NWs through the alloy catalytic tips, more than 10 tipped NW devices were identified with SEM. As illustrated in Fig. 2(a), the typical tipped device exhibits a gigantic resistance in dark due to the low intrinsic carrier concentration of grown NWs as well as the improper electrical contacts of the devices. However, upon illumination, these tipped devices exhibit obvious photovoltaic behavior with the measured current normalized to the light collection (channel) area of the NW rather than the cross-sectional area. This particular cell with the NW of 70 nm in diameter delivers a V_{oc} of ~ 0.6 V, a J_{sc} of ~ 11 mA/cm², and a fill factor (FF) of ~ 0.42 , which corresponds to an overall energy conversion efficiency of $\sim 2.8\%$ under AM 1.5 G illumination (100 mW/cm²). Although a Schottky barrier of ~ 0.6 eV has been recently reported by diffusing the Au atoms into the GaAs tip region,¹⁸ the associated NW Schottky barrier PV effect is observed in our experiment utilizing this efficient nanoscale Schottky formation between the GaAs NW and alloy Au–Ga catalytic tip. As a control experiment, similar asymmetric Ni/NW/Au device structures with the thermal evaporated electrodes were directly deposited on the bare NW, instead of the tip/NW nanocontacts, to obtain the Schottky interface. As shown in Fig. 2(b), the bare NW device exhibits a much smaller V_{oc} , J_{sc} , and efficiency due to the Fermi level pinning of GaAs NWs at both contacts, which is nearly independent of the work function of metal electrodes. As a result, only an inefficient and a small Schottky barrier is resulted in this asymmetric Ni/Au contact configuration yielding a poor PV effect, as compared with the tipped NW cell fabricated using the effective Schottky contact of Au–Ga alloy tip with GaAs NWs.

To further shed light on the mechanism of this NW Schottky barrier PV effect, energy band diagrams are schematically shown in Fig. 3 by comparing the tipped and bare GaAs NWs. Since there are abundant interface trapping states introduced by the surface oxide layer, the surface Fermi level is pinned near the intrinsic level (E_i) of NWs regardless of the work function of the metal electrodes. Also, as deduced from Fig. 2, the carrier concentration of grown NWs is found to be low as no intentional dopants were introduced in the NW synthesis. In this case, the energy difference between the Fermi

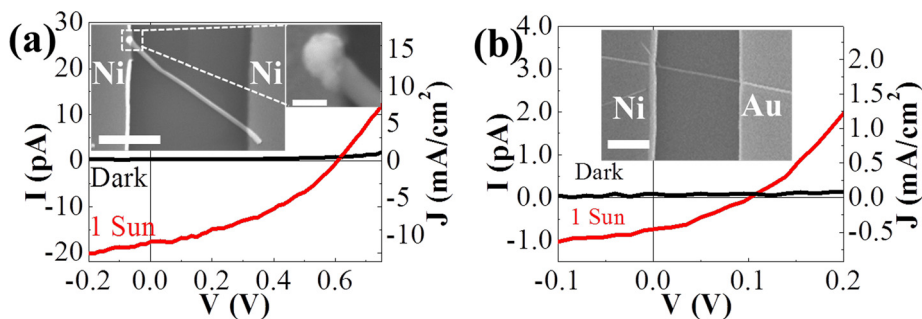


FIG. 2. Typical IV curves of the single GaAs NW photovoltaic device under dark and 1 sun illumination (AM1.5G, 100 mW/cm²) with the current density (J) normalized to the light absorption cross-sectional area (right axis). Insets show the corresponding SEM images of the devices. (a) The NW diameter is ~ 70 nm with the Au–Ga alloy tip (left) and Ni (right) as electrical contacts (scale bars are 1 μ m and 100 nm for the insets, respectively), and (b) the NW diameter is ~ 60 nm contacted with Au (left) and Ni (right) electrodes without any catalytic tip involved (scale bar is 1 μ m for the inset).

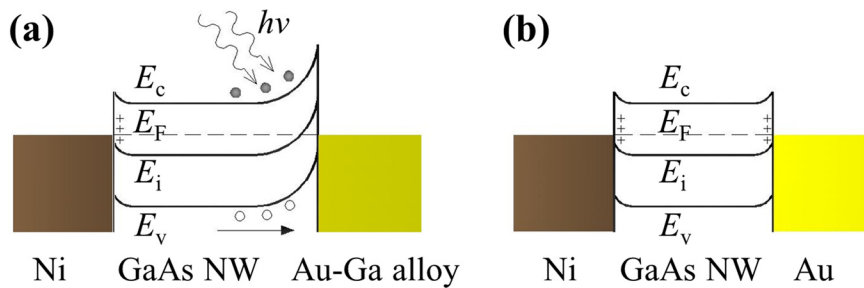


FIG. 3. The energy band diagrams of GaAs NW contacted with: (a) thermally deposited Ni and Au–Ga alloy tip, and (b) thermally deposited Ni and Au.

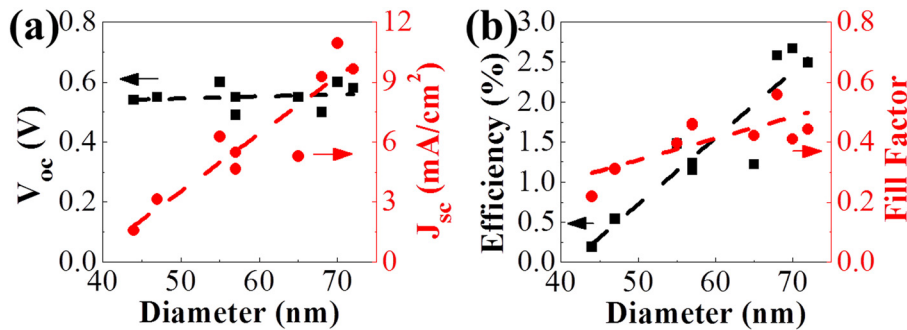


FIG. 4. Diameter dependence of the photovoltaic performance of single GaAs NW devices with the Au–Ga alloy tip and Ni as electrical contacts. (a) The open-circuit voltage (V_{oc}) and short-circuit current density (J_{sc}), and (b) the efficiency and FF as a function of NW diameters.

level (E_F) and E_i is relatively small; therefore, an inefficient and a small Schottky barrier (quasi-ohmic) is resulted when the bare GaAs NW is electrically contacted with either Ni or Au electrode (Fig. 3(b)). On the other hand, as shown in Fig. 3(a), when the GaAs NW is in nanoscale contact with its alloy Au–Ga catalytic tip, due to the presence of atomically abrupt interface with the minimized trap density, the surface E_F is believed to be de-pinned achieving an effective formation of Schottky barrier here. This way, a barrier height of ~ 0.52 eV can be purely estimated by $\Phi - (\chi + E_g/2)$, where Φ is the work function of Au (5.3 eV), χ is the electron affinity of GaAs (4.07 eV), and E_g is the bandgap of GaAs (1.42 eV),¹⁹ which is in good agreement with the observed V_{oc} for the tipped NW PV cell. The ability to readily obtain this efficient Schottky barrier formation with catalytic tips plays an essential role in achieving this superior PV performance of the tipped devices.

Meanwhile, when NW diameters of the tipped devices vary, both the J_{sc} and FF scale quasi-linearly and the V_{oc} stays relatively constant with the diameters (Fig. 4). It is mainly attributed to the reduced contact resistance and higher light absorption efficiency by larger diameter NWs while the Schottky height remains the same. Specifically, when the NW diameter is increased by $\sim 2\times$, the photon absorption (channel) area also goes up by $\sim 2\times$, but the total absorption volume is enlarged by $\sim 4\times$, assuming the thickness of NW is smaller than the photon penetration depth; therefore, the J_{sc} is expected to change linearly with the NW diameters. At the same time, when the NW becomes thicker, the influence of surface recombination becomes less significant for the less surface-area-to-volume ratio; therefore, it would result less surface-related leakage and the FF would increase accordingly. Notably, when the diameter is larger than 80 nm, no significant PV behavior is observed, and this is believed due to the large concentration of free electrons in

thick GaAs NWs,¹⁵ which degrades the photogenerated hole-current through recombination processes. Moreover, the PV efficiency is also found to scale inversely with the channel length as a result of the more surface recombination for the longer channels. All these experimental findings can demonstrate the uniform charge transfer and injection across the nanoscale contacts *via* catalytic tips. More importantly, it should be noted that this achieved efficiency ($\sim 2.8\%$) is comparable to the intentionally doped p–n junction GaAs NW solar cells,^{20,21} which further illustrates the advantages of this simple preparation method of GaAs NWs as well as the facile fabrication process of efficient NW Schottky barrier PV cells for the next generation high-performance, low-cost photovoltaics.

In summary, nanoscale Schottky contacts of GaAs NWs with their Au–Ga alloy catalytic tips are observed and utilized for photovoltaic devices. The corresponding NW PV cells are then fabricated with the best performance of $V_{oc} \sim 0.6$ V, $J_{sc} \sim 11$ mA/cm², FF ~ 0.42 , and efficiency $\sim 2.8\%$ for a NW diameter of 70 nm. The efficiency might be further improved by minimizing the inactive GaAs NW channel, suggesting the potency of this efficient Schottky barrier PV cell configuration in the large-area applications.

This work was supported by the Innovation and Technology Fund (ITS/049/10) from the Innovation and Technology Commission of the Government of the Hong Kong Special Administrative Region.

¹M. S. Gudiksen, L. J. Lauhon, J. Wang, D. C. Smith, and C. M. Lieber, *Nature (London)* **415**, 617 (2002).

²J. A. del Alamo, *Nature (London)* **479**, 317 (2011).

³K. Takei, T. Takahashi, J. C. Ho, H. Ko, A. G. Gillies, P. W. Leu, R. S. Fearing, and A. Javey, *Nat. Mater.* **9**, 821 (2010).

⁴R. X. Yan, D. Gargas, and P. D. Yang, *Nat. Photonics* **3**, 569 (2009).

⁵Z. Y. Fan, J. C. Ho, Z. A. Jacobson, R. Yerushalmi, R. L. Alley, H. Razavi, and A. Javey, *Nano Lett.* **8**, 20 (2008).

- ⁶A. I. Persson, M. W. Larsson, S. Stenstrom, B. J. Ohlsson, L. Samuelson, and L. R. Wallenberg, *Nat. Mater.* **3**, 677 (2004).
- ⁷B. A. Wacaser, K. A. Dick, J. Johansson, M. T. Borgstrom, K. Deppert, and L. Samuelson, *Adv. Mater.* **21**, 153 (2009).
- ⁸N. Han, A. T. Hui, F. Wang, J. J. Hou, F. Xiu, T. F. Hung, and J. C. Ho, *Appl. Phys. Lett.* **99**, 083114 (2011).
- ⁹F. Léonard and A. A. Talin, *Nat. Nanotechnol.* **6**, 773 (2011).
- ¹⁰N. Han, F. Y. Wang, A. T. Hui, J. J. Hou, G. C. Shan, F. Xiu, T. F. Hung, and J. C. Ho, *Nanotechnology* **22**, 285607 (2011).
- ¹¹X. W. Zhao, A. J. Hauser, T. R. Lemberger, and F. Y. Yang, *Nanotechnology* **18**, 485608 (2007).
- ¹²M. Ramdani, E. Gil, C. Leroux, Y. André, A. Trassoudaine, D. Castelluci, L. Bideux, G. Monier, C. Robert-Goumet, and R. Kupka, *Nano Lett.* **10**, 1836 (2010).
- ¹³M. Passlack, M. Hong, and J. Mannaerts, *Appl. Phys. Lett.* **68**, 1099 (1996).
- ¹⁴F. Jabeen, S. Rubini, F. Martelli, A. Franciosi, A. Kolmakov, L. Gregoratti, M. Amati, A. Barinov, A. Goldoni, and M. Kiskinova, *Nano Res.* **3**, 706 (2010).
- ¹⁵N. Han, F. Wang, J. J. Hou, F. Xiu, S. Yip, A. T. Hui, T. Hung, and J. C. Ho, *ACS Nano* **6**, 4428 (2012).
- ¹⁶N. Newman, W. Spicer, T. Kendelewicz, and I. Lindau, *J. Vac. Sci. Technol. B* **4**, 931 (1986).
- ¹⁷J. Woodall and J. Freeouf, *J. Vac. Sci. Technol.* **19**, 794 (1981).
- ¹⁸M. J. Tambe, S. Ren, and S. Gradečak, *Nano Lett.* **10**, 4584 (2010).
- ¹⁹D. R. Lide, *CRC Handbook of Chemistry and Physics*, 90th ed. (CRC, Boca Raton, 2010), pp. 12–114.
- ²⁰G. Mariani, P. S. Wong, A. M. Katzenmeyer, F. Léonard, J. Shapiro, and D. L. Huffaker, *Nano Lett.* **11**, 2490 (2011).
- ²¹J. A. Czaban, D. A. Thompson, and R. R. LaPierre, *Nano Lett.* **9**, 148 (2008).